Research on the Ultrasonic Welding of Titanium Alloy After Embedding Fiber Bragg Grating Sensor

Zhengqiang Zhu and Qiankun Xiao

Abstract Fiber Bragg grating (FBG) sensor is a preferred carrier for information transmission and sensing of smart metal structures. The electroplated nickel FBG is embedded in a direct or indirect way and welded by ultrasonic welding to research the rapid prototyping and sensing properties of the titanium alloy intelligent structural parts. The experiment of embedding electroplated nickel FBG into titanium alloy in the direct way shows that titanium alloy is not suitable for embedding matrix. The experiment of embedding electroplated nickel FBG in the indirect way shows that the figure of FBG temperature sensitivity is 2.13 times larger than that of original bare fiber grating, and is 1.11 times larger than that of direct way. This fact means that embedding metallized FBG into the titanium alloy structure in the indirect way is an effective way.

Keywords Metal intelligent structure · Embedded metal
Fiber Bragg grating (FBG)

1 Introduction

Owing to the unique properties, fiber Bragg grating (FBG) has been widely used in civil engineering, aerospace, shipbuilding, petrochemical and other fields [1]. In view of the advantages of energy conservation, environmental protection, easy operation and fast welding of ultrasonic welding [2], embedding FBG sensor into titanium alloy has a great research value to realize intelligent structure which can perceive the external environment [3]. Considering that the main component of ordinary fiber is quartz, and the strength especially the shear stress is poor, it becomes more fragile after coupling of the fiber grating sensor which is likely to cause damage to the fracture under the ultrasonic vibration [4, 5]. Therefore, it must

Z. Zhu (✉) · Q. Xiao
School of Mechanical & Electrical Engineering, Nanchang University, Nanchang, China
e-mail: zhuzhq01@163.com

S. Chen et al. (eds.), *Transactions on Intelligent Welding Manufacturing*,
Transactions on Intelligent Welding Manufacturing,
https://doi.org/10.1007/978-981-10-7043-3_6

be effectively protected before being embedded into titanium alloy. This paper introduces the metal protection method of FBG sensor in detail. Finally, the FBG is embedded according to the optimized process parameters of ultrasonic welding of titanium alloy, and the FBG embedded into titanium alloy is tested to determine whether it loses efficacy after being embedded [6].

2 Related Work on FBG

FBG is the most common fiber grating which belongs to the typical wavelength modulation type optical fiber sensor [7]. It uses the optical fiber writing technology to form a space phase grating with the core refractive index periodically changed along the fiber axes. The schematic diagram of the FBG sensor is shown in Fig. 1. When the broadband light wave transmits in the raster, the reflection of the light that satisfies the Prague phase matching conditions is strong, and the light that does not satisfy the Prague phase matching conditions is reflected back, while light transmission is not affected [8]. This is the choice of fiber grating light. Bragg was the first one to explain this tuning wavelength reflection phenomenon [9], so this kind of grating is named as Bragg grating, and the reflection condition is called Prague condition.

Due to the high melting point of the metal, the embedded fiber grating sensor has a lot of difficulties. The methods used are casting, shape deposition manufacturing, brazing and ultrasonic welding. In the casting method, Hamid et al. [10] cast a tin–lead alloy with a tin content of 65% (melting point of about 190 °C) in a square low carbon steel hollow model as a protective layer for optical fibers, and then used the laser free molding to deposit WC–Co alloy layer on the outer surface of the low carbon steel model. A high hardness outer cutting tool was obtained to monitor the temperature and stress of the tool during cutting. Figure 2 shows the FBG embedded cutting tool in the physical model. In the shape deposition manufacturing technology, a nickel-plated optical fiber sensor was successfully built into the stainless steel by laser-assisted shape deposition on the surface of the stainless steel

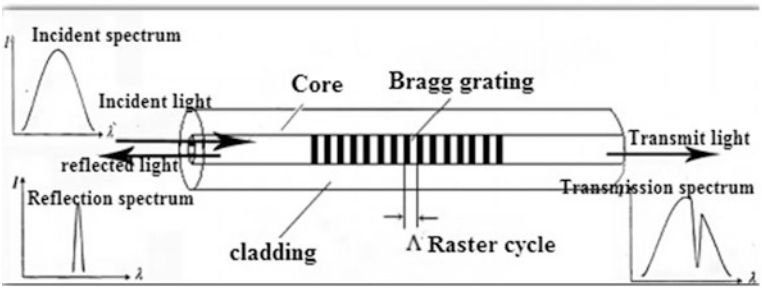

Fig. 1 Schematic diagram of FBG sensor

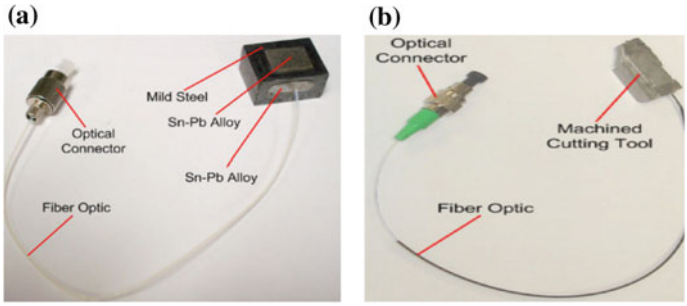

Fig. 2 The embedded FBG cutting tool in **a** the physical model by casting method and **b** laser free molding manufacturing method

substrate [11]. The FBG temperature sensitivity after the embedding was improved. In the brazing method, an electroplated nickel FBG was successfully buried into the low carbon steel, and the buried FBG temperature sensitivity increased by 1 times. In addition, a metal FBG was successfully crushed and embedded into the nickel-chromium alloy material by means of vacuum brazing, and the FBG temperature sensitivity increased by 1.1 times.

3 Experiments

3.1 Pretreatment

Fiber is a nonmetal. To coat the metal on its surface, it is necessary to make the fiber form a clean catalytic transition surface. The specific steps of the pretreatment are generally to remove the coating and then degrease and sensitize the final activation. After the pretreatment, it must plate nickel in the fiber to achieve further protection. Fiber grating plating nickel includes two steps: the first is chemical plating, and the second is electroplating.

Chemical plating refers to the catalytic reduction of metal ions in the bath on the substrate of the clean catalytic transition surface, and the reduced metal atoms are deposited on the surface of the substrate to form a continuous metal coating reaction process [12]. It has a lot of advantages, including uniform coating, beautiful appearance, a wide application of substrates (conductors, semiconductors and non-conductor), no-load current, and so on. The purpose of chemical plating nickel is to form a thin layer of conductive nickel-phosphorus alloy on the surface of the non-conductive fiber grating, and it is ready for electroplating nickel. Chemical plating experiment device is shown in Fig. 3.

Because of the nickel–phosphorus alloy layer is very thin after chemical plating, it is difficult to protect the fiber under high-frequency vibration grating. Therefore, it is necessary to electroplate a layer of dense nickel so as to improve the FBG's

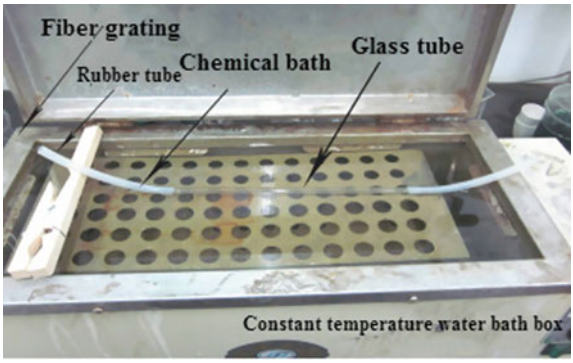

Fig. 3 Chemical plating device

anti-pressure and bending ability [13, 14]. Electroplating is an electro-chemical process that uses an electrolysis process to reduce the metal ions to metal and deposit them on the surface. Figure 4 shows the schematic diagram of fiber grating electroplating nickel.

Besides ultrasonic vibration, the welding temperature and welding pressure are also the key to embed FBG into titanium alloy under ultrasonic welding [15]. Therefore, it is important to design FBG sensor embedding method. We have designed two ways, named "direct embedding" and "indirect embedding". Figure 5 shows three kinds of direct embedding. Figure 6 shows a schematic diagram of indirect embedding scheme.

Considering that the thickness of the titanium alloy is 0.3 mm, the upper and lower titanium alloy is 0.6 mm totally. Therefore, the diameter of the FBG after the direct embedding method should be controlled within 0.6 mm. The FBG diameter of the nickel after plating is 300–550 μm (the diameter of the bare fiber is 125 μm).

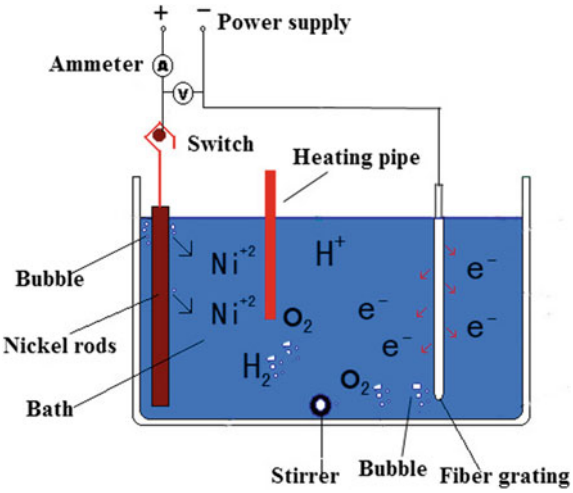

Fig. 4 Fiber grating electroplating nickel

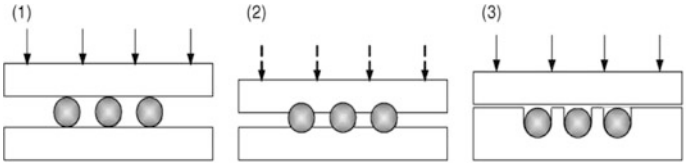

Fig. 5 Direct embedding FBG

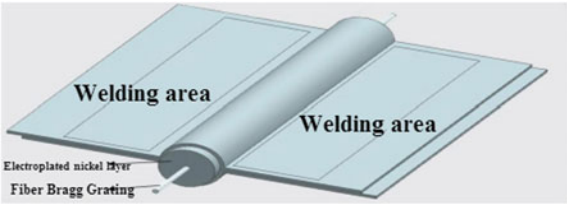

Fig. 6 Indirect embedding FBG

The indirect embedding method is not limited by the FBG diameter, and the thickness of the plating layer can be increased appropriately. The FBG embedded in the indirect way has a diameter of 841 μm after nickel plating. In three kinds of direct embedding, analysis shows that the second is more suitable for this experiment, as shown in Fig. 5.

3.2 Direct Embedding

Interception of Ti6Al4V titanium alloy sheet is completed by using the metal cutting equipment. The sheet is 150 mm × 40 mm × 0.3 mm. Three upper and lower grooves are machined into two titanium alloy sheets, as shown in Fig. 5. After the grooves are machined, alcohol is used to wipe the weld zone and groove to achieve a cleaner bonding surface and a better bonding strength. Adjust the ultrasonic welding equipment parameters. The use of ultrasonic welding parameters is: the operating frequency is 20 kHz, the maximum output power is 4 kW, the welding time is 45–125 ms, the vibration amplitude is 35 μm, the welding head area is 4 mm × 4 mm, and the welding pressure is 801.17, 1144.53 and 1487.89 N respectively. Some low hardness materials are used to position the weld before welding. The so-called positioning refers to no welding and no ultrasonic vibration, but the welding head under the welding pressure is in welding test. The purpose is to ensure the correct location of the welding [16]. Observe the indentation to determine whether the welding head plane is parallel to the base. Put the electroplated FBG into the groove between two flakes, and start pre-welding with a lower welding time. The purpose is to gradually bury FBG in the titanium alloy matrix, and to complete the final welding with the increase of the welding time.

3.3 Indirect Embedding

Interception of Ti6Al4V titanium alloy sheet is also completed by using the metal cutting equipment. The Ti6Al4V titanium alloy sheet is 150 mm × 20 mm 0.3 mm. With the machining method, the middle part of titanium alloy sheet is processed into the arc form that needs the plating of a good FBG arc and is processed into the arc close to coincidence to improve the FBG and titanium contact area. Then, the titanium alloy and FBG form an organic whole to protect the fiber grating. Figure 7 shows the arc area diagram. After processing of a good arc is completed, alcohol is used to wipe the welding area and arc area to obtain a cleaner surface and a better combination of bonding strength. The ultrasonic welding equipment parameters need to be adjusted. The optimization process parameters of the titanium alloy ultrasonic welding are: the operating frequency is 20 kHz, the maximum output power is 4 kW, the welding time is 125 ms, the vibration amplitude is 35 μm, the welding head area is 4 mm × 4 mm, and the welding pressure is 1144.53 N.

After pre-welding, put the plated FBG into the arc between two sheets. Weld one side of the arc first to reduce a subsequent welding impact on the previous welding area, and use mechanical method to clamp the welded area. Then, weld the other side. Welding should be careful to prevent the welding head from felling in the arc area.

3.4 Ultrasonic Welding

Ultrasonic metal welding [17, 18] as a special connection technology has lots of advantages, such as energy saving, environmental protection and easy operation. It has been widely used in the industrial field, especially in the electronics industry and nuclear energy industry for the preparation of new materials, body welding and parts packaging.

Ultrasonic metal welding principle is not transmitting the current to the material, and not applying the flame or arc and other high-temperature heat source to the material. It uses the ultrasonic high-frequency vibration and static pressure of the combined effect to clean the oxide film in the surface of material welding area. The ultrasonic high-frequency vibration energy enters into the material interface and brings the friction work, deformation energy and limited temperature rise to achieve the same metal or dissimilar metal connection in a special method [19, 20]. The schematic diagram of welding principle is shown in Fig. 8.

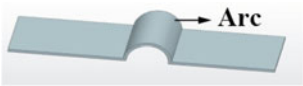

Fig. 7 Schematic diagram of arc area

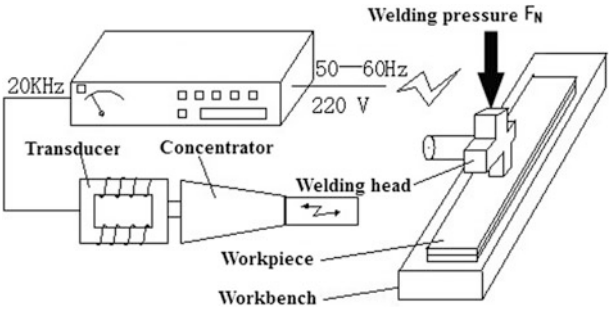

Fig. 8 Ultrasonic welding principle diagram

4 Results and Discussion

Embed the FBG sensor after metal protection into the titanium alloy structure directly, under the optimum welding process parameters (welding pressure is 1144.53 N and welding time is 125 ms). We accidentally find that FBG on both sides in the edge of the welding head is instantly cut into two sections at the end of welding [21]. By observing the cross-section and surface of the welded joints, we find that the joints of the upper and lower surfaces are smooth, and FBG embedding does not cause bulging. There is no pinhole on the cross-section due to the FBG embedded. The cross section is repeatedly observed by the metallographic microscope (magnification to 1000 times). Pinhole still cannot be found.

The welding time is gradually reduced. FBG still fails to be embedded. With the welding time at 105 ms and the welding pressure at 1144.53 N, the welding spot is peeled off. It is found that there is little black charred powder between the interfaces. Adjust the welding time at 85 ms or so. The titanium alloy ultrasonic welding is not reliable, so there is no need to further reduce the welding time. Figure 9 shows a cross-sectional view of the electroplated nickel fiber which is cut off at the edge of the weld with the welding pressure at 1144.53 N and the welding time at 85 and 95 ms respectively. When the welding pressure is reduced to 801.17 N, the

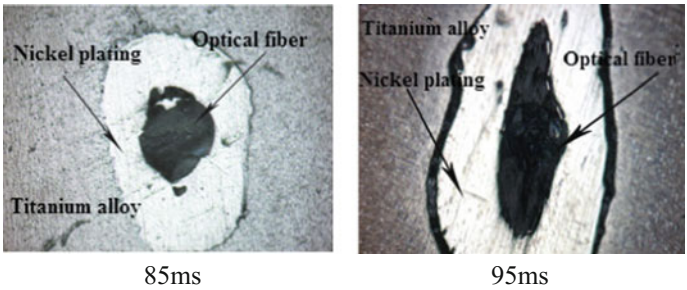

Fig. 9 A cross-sectional view of the nickel-plated fiber cut at the edge of the welding head

situation is similar as the welding pressure 1144.53 N. With lower welding time, electroplated nickel FBG is still flattened and the solder interface is not bonded. The main reason is that the titanium alloy has a high hardness, it is difficult to instantly press nickel plating FBG into the titanium alloy matrix, and the FBG is flattened by the welding pressure. Under the optimum welding process parameters, the interfacial temperature is as high as 1172.4 °C, while the nickel layer is too softened to protect the FBG at this temperature, and the yield strength is very low [22].

Considering the above reasons, the titanium alloy sheet is heated to 300 °C by incubator, and then the FBG is embedded, but the test indicates that there is no effect. Perhaps, the temperature needs to be heated to above 1000 °C, the titanium is completely softened, and then low welding energy FBG welding embedding may be successful. Due to the test equipment problems and considering that the FBG is not in the best welding process parameters, the welding embedding will lose the significance of the experiment, so the test stops.

After electroplated nickel FBG is embedded into the titanium alloy, its sensing performance is tested to determine whether the indirect embedding method is effective. Fiber grating sensing experiment equipment and fiber grating are produced by Shanghai Purple Light Photoelectric Technology Co., Ltd. The grating length is 32 mm, and the fiber grating Bragg center wavelength is 1550.103 nm at 20 °C.

Firstly, the temperature sensing test is taken for naked grating. Fiber coating stripping plier is used to strip the coating bare side layer of grating at a length of 15–20 mm. After stripping, wipe the fiber with cotton, put the fiber into the fiber adapter, then connect the light adapter in the fiber grating sensor network analyzer, and finally put the bare fiber grating into the constant temperature water bath box. Initial temperature is 20 °C and heated to 90 °C. The interval is 10 °C and stays 10 min. Record 15 reflection wavelengths when the wavelength becomes stable and take the average. The measured mean wavelength of the reflection is linearly fitted with Origin 8.5 software. Figure 10 shows the naked grating temperature sensor test data. We can see that the naked grating temperature sensor linearity is good from

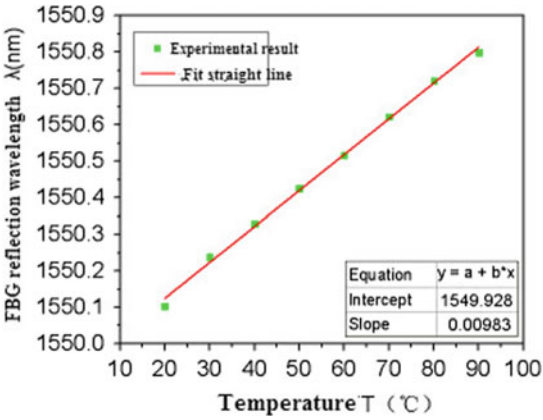

Fig. 10 Temperature measurement test data for bare fiber gratings

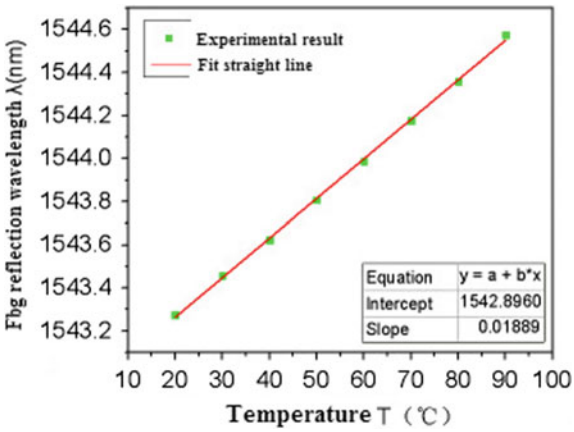

Fig. 11 Temperature sensing test data of electroplated fiber grating

the figure, and the intelligent metal structure of the information transmission is the ideal sensor. The fitting results show the temperature of the bare grating.

Metallize the bare fiber grating after the temperature sensing test, and test its temperature sensing. The purpose is to analyze the temperature sensitivity changes after the fiber grating embedded. The steps of the test are the same as those of the bare grating temperature sensing test. Figure 11 shows the temperature sensing test data of the electroplated fiber grating. It can be seen from the figure that the electroplated fiber grating maintains a good linearity. The temperature sensitivity of the electroplated fiber grating is 18.89 pm/°C. The temperature sensitivity has greatly improved than that of the original bare fiber grating.

Finally, make a temperature sensing test for the FBG embedded into titanium alloy in the indirect way. The test steps are the same as those of the bare grating temperature sensing test. Considering that the buried FBG has hysteresis phenomenon, so a set of temperature sensing tests for cooling down is added. Figure 12 shows the indirect embedded fiber grating temperature sensing test data. It can be seen from the figure that FBG reflection wavelength and temperature changes still maintain a good linear relationship, and there exists hysteresis phenomenon but it is not obvious. From the results of the fitting, it is found that the FBG temperature sensitivity coefficient in the titanium alloy structure is 20.92 pm/°C (during the temperature rise) and 20.71 pm/°C (during the cooling process). The temperature sensitivity has been improved before the fiber grating being embedded.

Due to the electroplated FBG or embedded FBG into the titanium alloy structure, the temperature sensitivity is improved. The reason is that the fiber grating is metallized or encapsulated, though the thermal coefficient of the fiber grating is not changed, but the metallized material or encapsulated FBG material thermal expansion coefficient is greater than the thermal expansion coefficient of fiber grating. The temperature changes play the role of thermal stress on the fiber grating, the grating center wavelength drift is exacerbated, so the fiber grating metallization or packaging increases the temperature sensitivity.

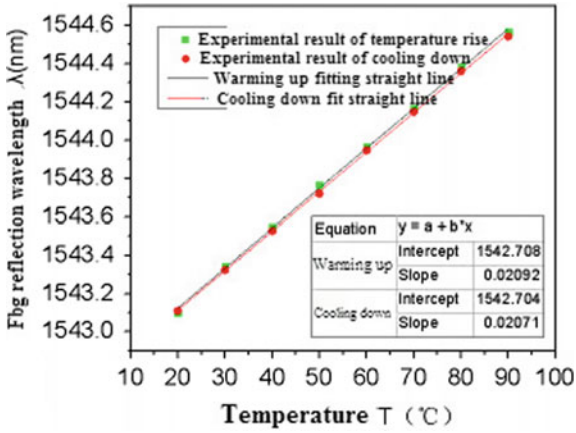

Fig. 12 Temperature measurement test data for FBG indirect embedding

The main parameters of FBG are provided by Shanghai Purple Light Photoelectric Technology Co., Ltd. The specific parameters are: Poisson's ratio is 0.17, thermal expansion coefficient is 0.55×10^{-6} °C^{-1}, elastic modulus is 7.474 kPa, thermal coefficient is 667.8 °C^{-1}, center wavelength is 1550.103 nm, elastic coefficient is 0.121 and 0.27, and fiber grating diameter is 125 μm. The nickel plating layer parameters are: thermal expansion coefficient is 1.42×10^{-5} °C^{-1}, Poisson's ratio is 0.31, and elastic modulus is 1981.56 Pa.

$$\frac{\Delta\lambda_B}{\Delta T} = (a_0 + \zeta)\lambda_B + \left\{D - \frac{n_{eff}^2}{2}\left[(P_{11} + P_{12})C + P_{12}D\right]\right\}\lambda_B \tag{1}$$

$$D = \frac{(a_1 - a_0)E_1[B - 2v_0]}{B\left(E_0\frac{S_0}{S_1} + E_1\right) - 2E_1v_0 - 2E_0v_1\frac{S_0}{S_1}} \tag{2}$$

$$C = \frac{(a_1 - a_0)E_1[(1 - v_0) - Bv_0]}{B\left(E_0\frac{S_0}{S_1} + E_1\right) - 2E_1v_0 - 2E_0v_1\frac{S_0}{S_1}} \tag{3}$$

$$B = 1 + \frac{(S_1 + S_0)(1 + v_1)E_0}{E_1(1 + v_0)S_1 + E_0(1 + v_1)S_0} \tag{4}$$

where a_0 is the thermal expansion coefficient of optical fiber, a_1 is the thermal expansion coefficient of Nickel plating, ζ is the optical fiber thermal coefficient, v_0 is the fiber Poisson ratio, v_1 is the Poisson's ratio of the nickel-plated layer, S_0 and S_1 are fiber grating cross-sectional area, E_0 is the elastic modulus of the fiber, E_1 is the elastic modulus of the nickel plating layer, P_{11} and P_{12} are shelling coefficients, λ_B is the center wavelength of the grating, and n_{eff} is the effective refractive index of the fiber. The thickness of the coating 358 μm and above parameters are taken into Eq. (1). The theoretical value of FBG temperature sensitivity is 20.91 pm/°C, while

the measured value is 18.89 pm/°C. There is no big difference between the theoretical value and the actual value. The main reason is that there is deviation in the calculated parameters and the actual parameters used.

5 Conclusion

The test of embedding electroplated nickel FBG into the titanium alloy in the direct way means that the titanium alloy is not suitable for embedding matrix. The temperature sensitivity coefficient of the bare fiber grating is 9.83 pm/°C, and the sensitivity of FBG is 18.89 pm/°C after nickel plating. The FBG temperature sensitivity coefficient of the indirect embedding into titanium alloy structure is 20.92 pm/°C (during the temperature rise) and 20.71 pm/°C (during cooling). The temperature sensitivity of the FBG embedded into the titanium alloy in the indirect way is 2.13 times larger than that of the original bare fiber grating, and is 1.11 times larger than that of the FBG sensor after electroplating nickel. It indicates that indirect embedding is an effective method to embed FBG into the titanium alloy structure. FBG is not damaged by indirect embedding into the titanium alloy, and the temperature sensitivity has been improved.

References

1. Othonos A, Kalli K, Pureur D et al (2006) Fibre Bragg gratings. Springer, Berlin, pp 189–269
2. Hill KO, Meltz G (1997) Fiber Bragg grating technology fundamentals and overview. J Lightwave Technol 15(8):1263–1276
3. Studer M, Peters KJ (2017) Embedded optical fiber Bragg grating sensors for the measurement of crack-bridging forces in composites. Proc SPIE Int Soc Opt Eng 4694:284–295
4. Peng PC, Tseng HY, Chi S (2014) Long-distance FBG sensor system using a linear-cavity fiber Raman laser scheme. IEEE Photonics Technol Lett 16(2):575–577
5. Jin L, Zhang W, Zhang H et al (2005) An embedded FBG sensor for simultaneous measurement of stress and temperature. IEEE Photonics Technol Lett 18(1):154–156
6. Wang X, Matsushima K, Nishiki A et al (2004) High reflectivity superstructured FBG for coherent optical code generation and recognition. Opt Express 12(22):5457–5468
7. Lau KT, Yuan L, Zhou LM et al (2011) Strain monitoring in FRP laminates and concrete beams using FBG sensors. Compos Struct 51(1):9–20
8. Leng J, Asundi A (2003) Structural health monitoring of smart composite materials by using EFPI and FBG sensors. Sens Actuators, A 103(3):330–340
9. Lancet T (1942) Sir William Bragg. Lancet 239:360
10. Hamid RK, Mauricio Z, Ningsu L (2010) Application of adaptive wavelet networks for vibration control of base isolated structures. Int J Wavelets Multiresolut Inf Process 08 (05):773–791
11. Yu X, Yu Y, Liao Y et al (2005) Strain measurement of steel structure using a novel FBG sensor packaged by titanium alloy slice. Proc SPIE 6019:448–453
12. Jing W, Hou W (1996) Chemical plating. J Yanbei Teach Coll 12(4):32–34
13. Bladon JJ (1995) Electroplating process. US Patent 5425873 A

14. Liang W, Huang Y, Xu Y et al (2005) Highly sensitive fiber Bragg grating refractive index sensors. Appl Phys Lett 86(15):151122
15. Pospori A, Marques CAF, Sáez-Rodríguez D et al (2017) Thermal and chemical treatment of polymer optical fiber Bragg grating sensors for enhanced mechanical sensitivity. Opt Fiber Technol 36:68–74
16. Takeda S, Minakuchi S, Okabe Y et al (2015) Delamination monitoring of laminated composites subjected to low-velocity impact using small-diameter FBG sensors. Compos A Appl Sci Manuf 36(7):903–908
17. Zhang CQ, Robson JD, Prangnell PB (2016) Dissimilar ultrasonic spot welding of aerospace aluminum alloy AA2139 to titanium alloy TiAl6V4. J Mater Process Technol 231:382–388
18. Lipari CP (1983) Ultrasonic welding. US Patent 4410383 A
19. Watanabe T, Sakuyama H, Yanagisawa A (2009) Ultrasonic welding between mild steel sheet and Al-Mg alloy sheet. J Mater Process Tech 209(15–16):5475–5480
20. Harman G, Albers J (2003) The ultrasonic welding mechanism as applied to aluminum-and gold-wire bonding in microelectronics. IEEE Trans Parts Hybrids Packag 13(4):406–412
21. Matsuoka SI (1998) Ultrasonic welding of ceramics/metals using inserts. J Mater Process Technol 75(1–3):259–265
22. Panteli A, Robson JD, Brough I et al (2012) The effect of high strain rate deformation on intermetallic reaction during ultrasonic welding aluminium to magnesium. Mater Sci Eng, A 556:31–42